*CHAPTER - 1*

# INTRODUCTION

## 1.1 CONCEPT OF REMOTE SENSING

Remote sensing is the science and technology of acquiring information and monitoring the dynamical changes on Earth surface features by measuring its reflected and emitted electromagnetic radiation (EMR) without being in any physical contact (typically from the space-borne or air-borne platform). However, the remote sensing data about the object, area, or any phenomenon must be accessible and could be transferred from the place of observation to the processing and analysis unit. It is usually done by using microwaves, infrared, and visible rays of the electromagnetic spectrum to acquire information about the Earth target under investigation for remote sensing purposes. Therefore, it is equally important to understand the physics of EMR and how it interacts with the Earth targets, not just with the target, but also with the atmospheric constituents (scattering, absorption and transmission) through which it travels (Figure 1.1). The remote sensing theory and techniques totally depends on the knowledge of the interaction of EMR with the different Earth surface targets and the development of new satellite sensors for the effective management of resources for mankind.

After the generalization of optical theories of the sensors, the word remote sensing was first introduced in 1960s (before it was known as aerial photography). In 1970s the National Aeronautics and Space Administration (NASA) and United States Geological Survey (USGS) jointly launched the LANDSAT satellite under the Earth observation mission. Now, the LANDSAT - 8 (OLI) satellite is operationally orbiting for the Earth observation in the visible and infrared regions (0.43 to 12.5 μm). The first Indian remote sensing (IRS) satellite mission was launched in 1988 by Indian Space research Organisation

(ISRO). Subsequently, the various optical and synthetic aperture radar (SAR) satellite missions are working operationally in space platform (Resourcesat-1/2, Cartosat, Oceansat-2 and RISAT-1/2).

In the mid-1950s, the theory of SAR technology was developed to capture the remote sensing images in microwave regions (1mm to 1m). The SAR sensors provide the high-resolution imagery from the high-flying aircraft or space platform. Currently, the various well known SAR sensors are operationally working in the different microwave regions with high spatial resolution and having frequent revisit time at same location on the Earth surfaces. The Sentinel - 1A, RADARSAT - 1/2, ALOS -PALSAR – 1/2, TerraSAR - X and RISAT - 2 are the working mode SAR remote sensing satellite missions for the Earth observations.

The potential of remote sensing satellites has increased rapidly for the application of various activities at Earth surfaces over the past two decades. Due to availability of fine spatio-temporal satellite images, the number of methodologies has grown to study the agricultural, urban and meteorological applications.

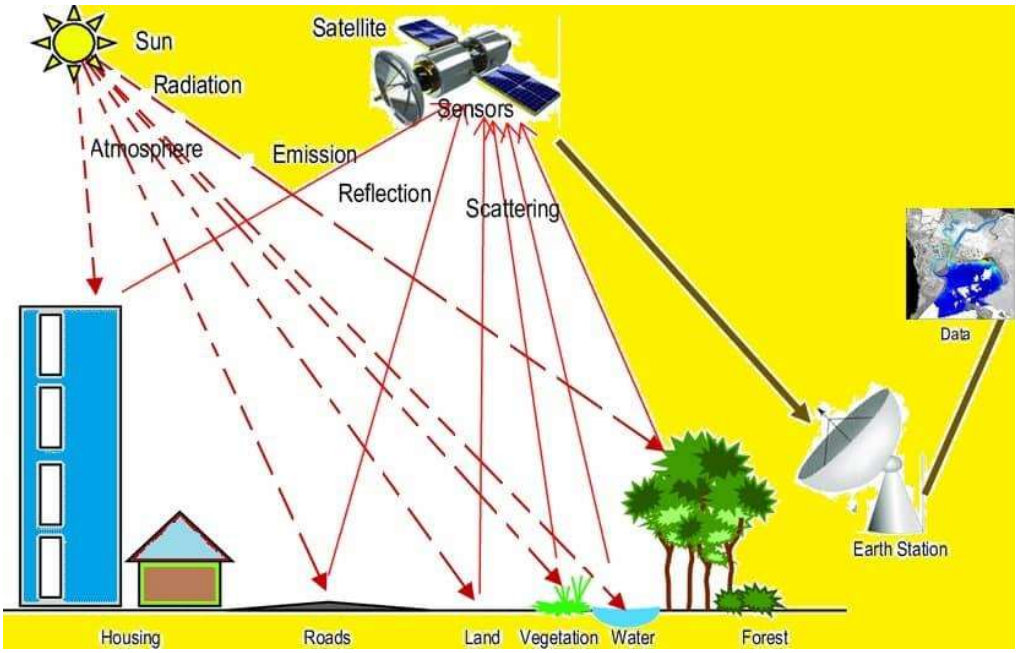


**Figure 1.1.** Remote sensing imaging process of Earth targets

(**Source:** https://gisrsstudy.com/wp-content/uploads/2020/08/Remote-Sensing.jpg)

## 1.2 TYPES OF REMOTE SENSING

Depending upon the source of illumination, remote sensing is further categorized into two ways: **Active** and **Passive** remote sensing. Figure (1.2) shows the active and passive remote sensing mechanism for source of illuminating energy and collecting the reflected parts of energy from the target of interest.

### 1.2.1 Passive remote sensing

In the passive remote sensing, the source of energy is from natural way or Sun is used to illuminate the target of interest. The Sun is one of biggest source of natural energy for passive remote sensing. When the sun is illuminating the EMR on the Earth targets, reflected energy is recorded by the passive sensor. During night time, the passive sensors are not able to record the reflected energy from the Earth targets because the Sun is not illuminating the Earth targets. The gamma ray spectrometer, aerial camera, radiometer and thermal scanner are the example of passive remote sensing.

### 1.2.2 Active remote sensing

Active remote sensing techniques have their own source of radiant energy for illuminating the Earth target under investigation. The reflected EMR energy from the target is detected and recorded by the active sensors. Active sensors have great advantages to sense the Earth surfaces during both day and night time. Also, active sensors can sense the Earth features in any weather conditions. Unlike the passive sensors, the active sensor records the reflected energy coming from the Earth surface in the microwave regions. The most familiar example of active sensors are RADAR, LIDAR, Scatterometer, RADAR altimeters and synthetic aperture radar (SAR).

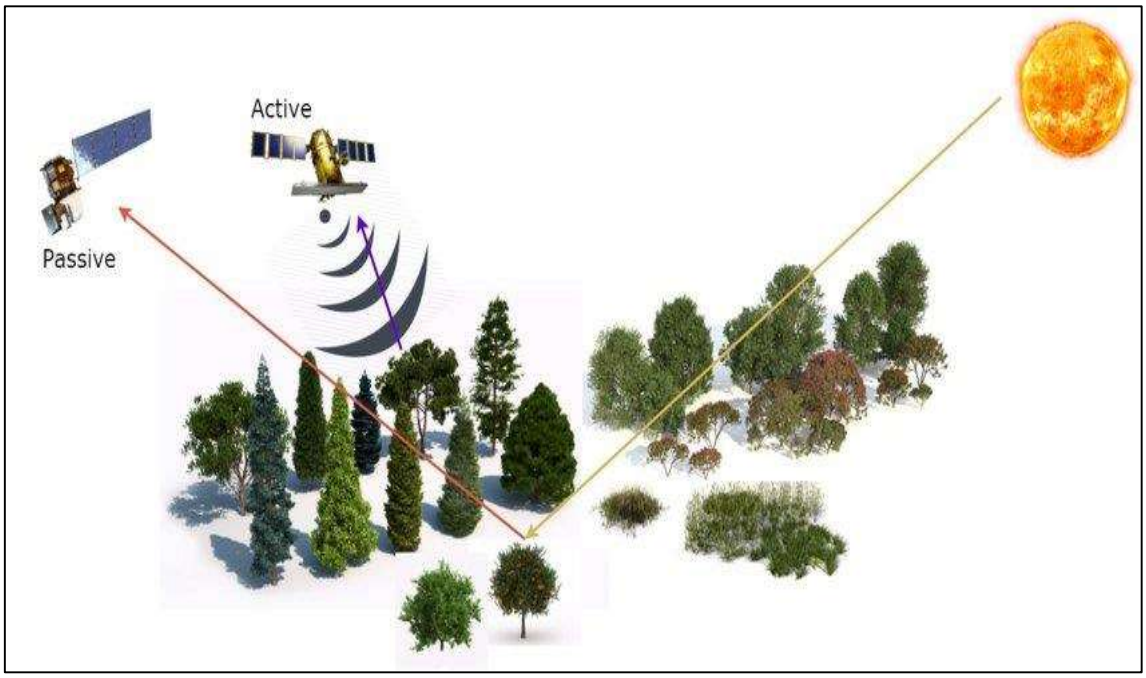


**Figure 1.2** Remote sensing illuminating process (Passive and Active remote sensing)

(**Source**: M. Campos-Taberner, 2017)

## 1.3 INTERACTION OF ELECTROMAGNETIC RADIATION (EMR) WITH ATMOSPHERE AND MATTER

### 1.3.1 Interaction of EMR with the atmosphere

The EMR from the Sun or remote sensing satellite sensors travels some distance in the atmosphere before radiation reaches the Earth surface. The atmospheric constituents (particles and gases) can affect the incoming radiation. These effects are caused by the three mechanisms: **scattering, absorption** and **transmission.**

#### 1.3.1.1 Scattering

Atmospheric scattering phenomena take place when EMR interacts with particles and large gas molecules causing its path to redirect from its original path. The atmospheric scattering is a function of many factors such as the wavelength, density and size of particles or gas molecules. Further, the scattering phenomenon is categorized into three types: (I) **Rayleigh scattering** (II) **Mie scattering** and (III) **Non - selective scattering**.

**(I) Rayleigh scattering**

Rayleigh scattering takes place when the sizes of particles or gas molecules are very small as compared to incident EMR. The Rayleigh scattering primarily caused by air particles, such as nitrogen, and oxygen molecules, are much smaller than the wavelength of the incoming radiation. Also, this scattering is wavelength dependent and its scattered intensity is inversely proportional to $\lambda^{-4}$ . The occurrence of blue colour sky is caused by Rayleigh scattering because the blue colour (shorter wavelength) of the visible spectrum gets scattered more than the other longer wavelengths.

**(II) Mie scattering**

Mie scattering occurs when the incident EMR wavelength is comparable or similar in size of the atmospheric particles. These are caused by aerosols: a mixture of gases, water vapour and dust. Mie scattering dominates in the lower parts of the atmosphere, where the larger particles are abundant and dominates under overcast cloud conditions. It influences the entire spectral region from ultra violet to near infrared regions. The Mie scattering is wavelength dependent ($\lambda^0$ to $\lambda^{-4}$ ).

**(III) Non - selective scattering**

The Non- selective scattering takes place when the particle size is much larger than the wavelength of the incident EMR. The water droplets and larger dust particles are responsible for such type of scattering. This scattering is independent of the wavelength ($\lambda^0$) and all the wavelength are equally scattered. The most common example is the appearance of fog and clouds as white to human eyes caused due to non-selective selective scattering since the scattering of blue, green and red light is of same intensity (blue + green + red = white).

### 1.3.1.2 Absorption

The absorption is the process when the incoming source of EMR partly is absorbed by the atmospheric constituents. The primary atmospheric constituents are the Ozone ($O_3$), carbon dioxide ($CO_2$), and water vapour ($H_2O$) which causes the effective loss of EMR intensity at a specific wavelength.

Moreover, Ozone ($O_3$) absorbs the harmful ultraviolet radiation coming from the sunlight preventing it to reach the Earth's surface. The human skin can burn when exposed to sunlight in the absence of this protective ozone layer. The carbon dioxide ($CO_2$) causes the greenhouse effect. Thus, it is also known as a greenhouse gas. If there were no greenhouse gases in the atmosphere, then the average value of Earth's surface temperature would be approximately -18 °C as compared to present average value of 15 °C. Since, it strongly absorbs the far IR portion of the electromagnetic spectrum and then reemits it as heats, which keep the Earth's surface objects warm by trapping this heat within the atmosphere. Water vapour present in the atmosphere causes absorption in the long wave IR and some part of microwave regions.

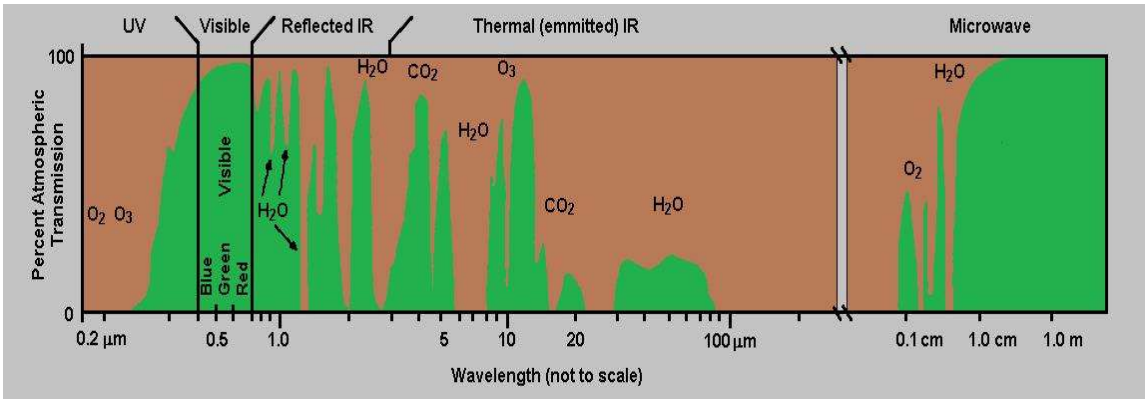


**Figure 1.3** Atmospheric transmittance (atmospheric window)

(**Source:**http://employees.oneonta.edu/baumanpr/geosat2/RS-Introduction/RS-Introduction.html)

However, the atmospheric molecules absorb incoming EMR energy in particular wavelength regions of the electromagnetic spectrum. For remote sensing purposes, the wavelength regions useful must be transparent to the atmospheric constituents. These regions of the EMR spectrum are known as **atmospheric windows**. In the Figure 1.3, the green parts show suitable wavelengths regions of electromagnetic spectrum which are useful for remote sensing satellite acquisition at the Earth surfaces. The atmospheric window consists of windows channels 0.4 to 0.7 μm in visible and 0.7 to 14 μm in the NIR and thermal IR region of the electromagnetic spectrum (discrete wavelength intervals). Whereas, there is large atmospheric window available in the microwave regions (1 mm to 1 m).

#### 1.3.1.3 Transmission

Transmission of EMR occurs when radiation passes through a substance without significant attenuation (scattered and absorbed). For a given thickness, or depth of a substance, the ability of a medium to transmit energy is measured as transmittance (τ).

$$\tau = \frac{\text{Transmitted radiation } (E_T)}{\text{Incident radiation } (E_I)}$$

### 1.3.2 Interaction of EMR with the matter (Earth surface)

The EMR which is not influenced (absorbed or scattered) by atmospheric particles and gases can arrive the Earth surface and interact with targets. There are a number of ways in which EMR can interact with land surface features depending on the wavelength of incident radiation and on the nature of targets (smooth or rough surface). When EMR interact with the Earth features, all the energy is conserved as the total amount of energy dissipated by reflection ($E_R$), transmission ($E_T$) and absorption ($E_A$) equals the incident energy ($E_I$). Therefore, we can write

$$E_I = E_R + E_A + E_T \qquad (1.1)$$

Dividing Equation (1.1) by incident energy ($E_I$), gives

$$\frac{E_I}{E_I} = \frac{E_R}{E_I} + \frac{E_A}{E_I} + \frac{E_T}{E_I} \quad (1.2)$$

This equation can be written as

$$\rho + \alpha + \tau = 1 \quad (1.3)$$

Where ρ, α and τ are defined as the reflectance, absorptance and transmittance of the Earth target features, respectively. The fractions of incident EMR energy that is in term of reflected, absorbed and transmitted depend upon the nature of the Earth surface features and its condition. For example, interaction at optical and thermal wavelengths takes place mainly through the electric field vector in EMR that causes electronic and vibrational transitions in the material. In the case of microwaves, it is the dipole moment (dielectric constant) of the vegetation and soil materials that determine the intensity of the interaction. Notably, these three parameters are also wavelength dependent, and so the relative amount of intensity reflected, absorbed, or transmitted vary with the wavelength in vegetation or soil regions.

## 1.4 CHARACTERISTICS OF REMOTE SENSING IMAGE

The optical and microwave remote sensing image quality depends on the sensor properties and the distance of the Earth's surface features from the space-born satellite platform. There are four types of resolution which helps to categorize the image quality i.e. spatial, spectral, radiometric and temporal resolution.

### 1.4.1 Spatial resolution

The spatial resolution refers to the identification of smallest feature size by the sensor at the Earth surfaces. All the objects on Earth surface which has dimension greater than that of the spatial resolution of a particular sensor can be detected by that sensor. The spatial resolution primarily depends on their Instantaneous Field of View (IFOV) for passive sensors and the altitude of the platform containing sensor from the Earth surface. The solid angle through which a sensor can detect the EMR from the Earth surface is known as IFOV. The

multiplication of the IFOV and the altitude of sensor determines the area on the Earth surface as seen by the sensor at a particular moment of time. The Figure 1.4 shows three images of BHU campus at three different spatial resolutions of 5.8 m, 30 m and 56 m. It can be observed that the smaller features can be identified in the image with 5.8 m resolution as compared to that of 30 m and 56 m resolution images.

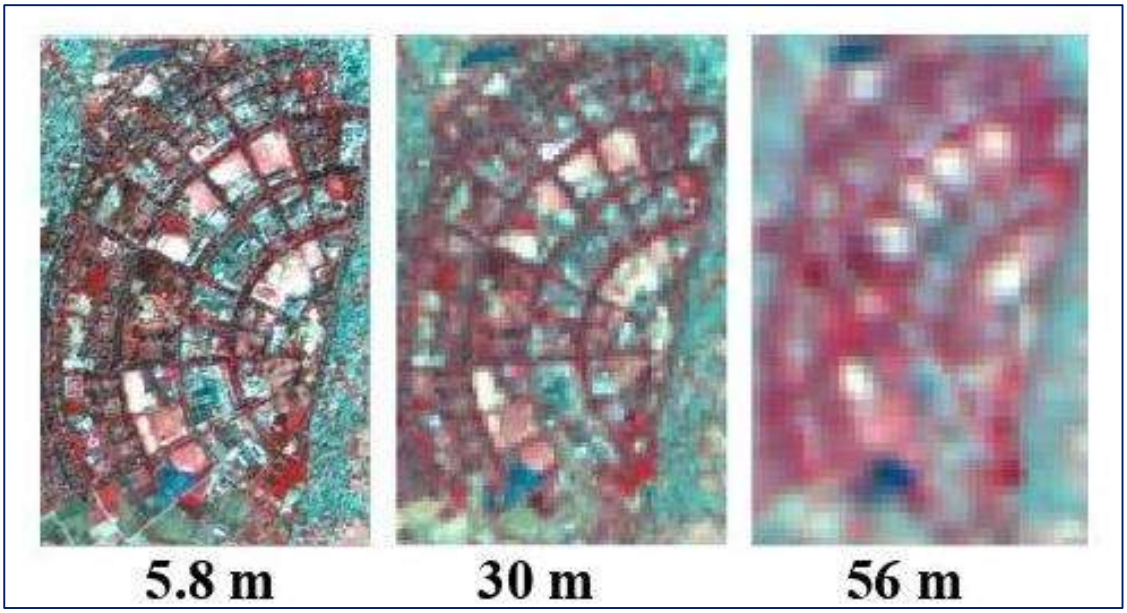


**Figure 1.4** The location of Banaras Hindu University campus at 5.8 m, 30 m and 56 m spatial resolution

### 1.4.2 Spectral resolution

The Spectral resolution refers to the ability of a sensor to determine finer wavelength intervals or to resolve the electromagnetic energy received in a spectral wavelength ranges to distinguish the different components of the Earth surface. Various remote sensing sensors records energy at different wavelength intervals and different features or details about the features on Earth surface can be distinguished by analysing the spectral response at different wavelength ranges. The multi-spectral sensors can be useful for distinguishing broad land cover classes like vegetation, soil, water etc. Therefore, the hyperspectral sensors provide

reflectance at very fine wavelength intervals which helps for fine study like types of rocks, types of crop, vegetation health or stress, water quality etc. The hyperspectral data (AVIRIS, HySI and Hyperion) may provide more than 100 bands with a narrow bandwidth of 5 to 10 nm whereas the multi- spectral data (Landsat -8, LISS -IV and Sentinel -2) provides 3 to 13 bands with a broader bandwidth of 70 to 400 nm in the visible and IR portions of the electromagnetic spectrum.

### 1.4.3 Radiometric resolution

The radiometric resolution refers to the potential of the sensor to distinguish small differences in electromagnetic energy that reaches the sensor from the Earth surface. It is measured through the number of grey level values. The sensor with finer radiometric resolution is more sensitive to distinguishing the fine differences in reflected or emitted energy. The grey level of satellite images can be varying from 0 to $2^n$-1, where n is the number of bits. The radiometric resolution of an image can be represented as number of bits or binary numbers. Thus, the 2-bits image has 4 brightness levels, 8 -bits image has 256 brightness levels, 16-bits image has 65536 brightness levels. For example, the radiometric resolution of some common satellite sensors are LISS -IV (10 -bits), Landsat-8 (12-bits) and Sentinel -1 A (16-bits).

### 1.4.4 Temporal resolution

The temporal resolution is defined as the revisit time of the satellite sensors at the exactly same position on the Earth surface. The spectral characteristics of the vegetation or other surface features at a same geo-location may change with time. The fine multi-temporal satellite imagery helps us to do more accurate study about the differences occurred on the Earth surface at same geo-location in a specific time interval for various application like floods, Earthquake, forest fire and some high-risk disaster events. For the purpose of

vegetation remote sensing, the multi-temporal images can be more useful for the study of crop growth stages, crop stress, crop irrigation practices and drought conditions in vegetative areas. Temporal resolutions of some common satellite sensors are LISS - IV (24 days), Landsat - 8 OLI (16 days), Sentinel - 1A (12 days), ALOS - 2 (14 days) and Sentinel - 2 (10 days) .

## 1.5 SPECTRAL SIGNATURE OF VEGETATION AND SOIL

The spectral signature signifies the curve between reflectance values and wavelength. At the surface of Earth, every material has its own spectral signature curve. The most abundant features are vegetation and soil surfaces. Both vegetation and soil have unique spectral reflectance curves. A typical spectral reflectance curves for three basic Earth features like vegetation, soil and water are shown in Figure 1.5. Chlorophyll strongly absorbs light at wavelengths around 0.45 (blue) and 0.67 μm (red) and creates more fuel for the vegetation. Whereas, it reflects strongly green light because our eyes perceive healthy vegetation as green. Therefore, more fuel means high level of chlorophyll content (healthy) and have a high reflectance value in the near-infrared (NIR) between 0.7 and 1.3 μm spectral regions. However, if vegetation has stress and dead conditions then leaves are not making fuel sufficiently which causes decrease in the chlorophyll content and resulting low reflectance values appearing in NIR region (Figure 1.6). As this internal structure varies amongst different crop leaves, the near infrared wavelengths can be used to discriminate between different crop species.

The water (liquid state) has comparatively low reflectance value, with clear water having the high reflectance value in the blue portion (0.45 μm) of the visible part of the electromagnetic spectrum. Water has high absorption and virtually no reflectance in near infrared wavelengths range and microwave spectral regions. Turbid water has a higher

reflectance in the visible region than clear water. This is also true for waters containing high chlorophyll concentrations.

The bare soil, having least amount of water, generally shows higher reflectance value in NIR and short-wave infrared (SWIR) region. Whereas, the wet soil (high percentage of water) relatively lowers the reflectance value due to water absorption. Since, water absorbs almost all the incoming EMR energy at the wavelength longer than 0.75 µm. Generally, the rough surface reflects less, due to self-shadowing effects and multiple scattering. Also, the soil reflectance value prominently affected by the following factors:

- Moisture content
- Soil texture (proportion of sand, silt, and clay)
- Surface roughness
- Presence of iron oxide
- Organic matter content

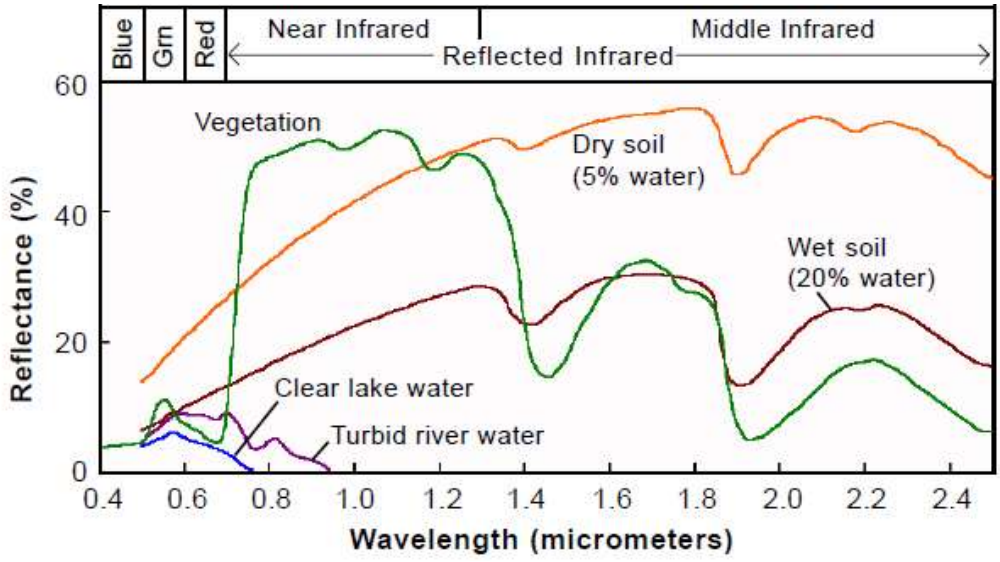


**Figure 1.5** Spectral reflectance curve for vegetation, soil and water

(**Source:** https://www.researchgate.net/profile/Saba_Daneshgar2/ Typical-spectral-signature-of-different-surfaces-wwwmicroimagescom.png)

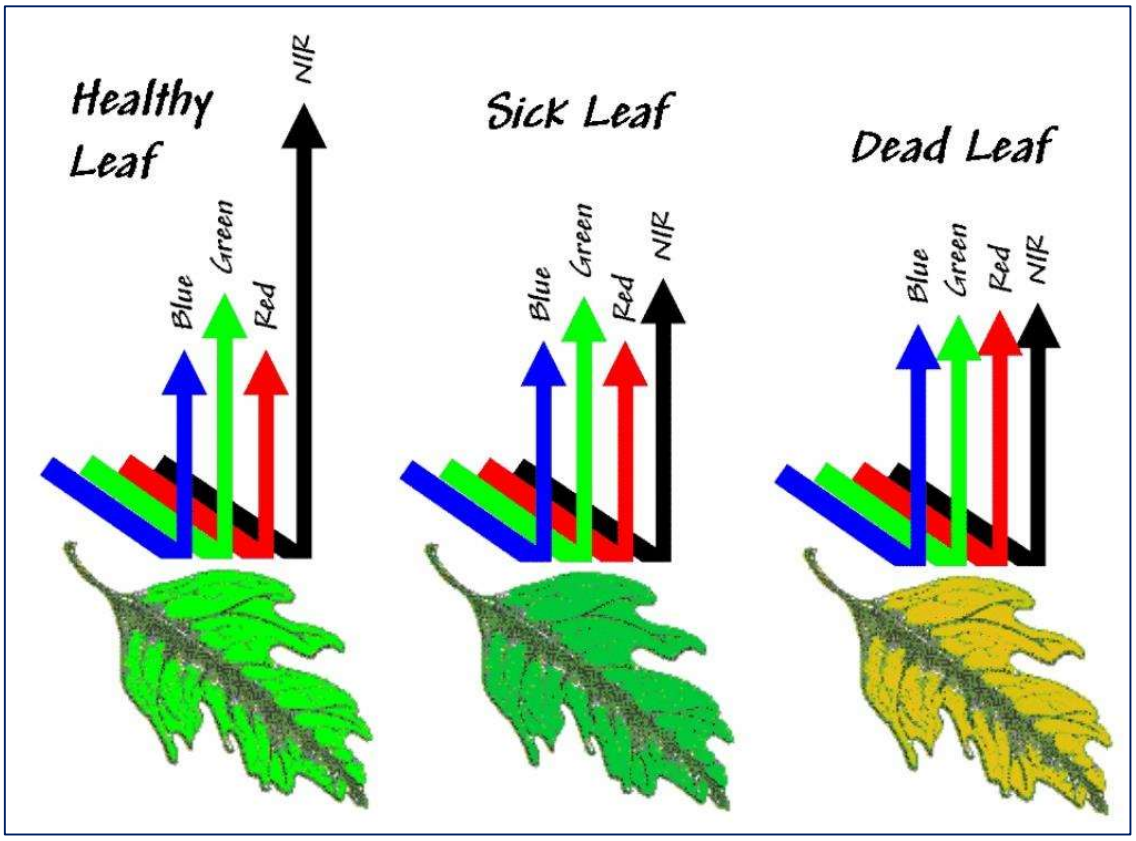


**Figure 1.6** The spectral reflectance of vegetation leaves for healthy, sick and dead conditions

## 1.6 SPECULAR AND DIFFUSE SURFACE SCATTERING

The specular and diffuse scatterings are the phenomenon of regular and irregular backscattering echoes directions. During crop growth seasons, the vegetative and bare soil surfaces are primarily rough. The larger is the roughness parameters of the soil surfaces, the higher are the backscattering signal of electromagnetic wave incidents on it. Therefore, the SAR data for rough surface pixels shows brighter in the images. However, the backscattering echoes of the incident electromagnetic wave from the rough soil surface is dependent upon the surface roughness parameters, which rely on the frequencies of the incident electromagnetic wave, polarization and local incidence angle. The, root mean square height $(s)$ and autocorrelation length $(l)$ are two major parameters which characterize the roughness conditions of soil surfaces.

The electromagnetically, Rayleigh and Fraunhofer criteria are greatly utilized for the classification of smooth (specular reflection) and rough (diffuse reflection) surface as shown in Figure 1.7. When the plane electromagnetic signal is incident on the bare surface at a local incidence angle (θ), then the phase difference (Δϕ) introduced to two backscattered electromagnetic signals from the separate points on the surface decides the surface to be smooth or rough. It can be determined by using Equation (1.4) as below

$$\Delta\phi = 2s\,\frac{2\pi}{\lambda}\cos(\theta) \qquad (1.4)$$

**(I)** In Rayleigh criteria, if the phase difference ($\Delta\phi$) between two the backscattered waves is less than $\frac{\pi}{2}$ radian, then the surface appears to be as smooth i.e.

$$s < \frac{\lambda}{8\cos(\theta)} \qquad (1.5)$$

**(II)** In Fraunhofer criterion, being more stringent criterion, the surface appears to be as smooth, if the phase difference is less than $\frac{\pi}{8}$ i.e.

$$s < \frac{\lambda}{32\cos(\theta)} \qquad (1.6)$$

Mostly, the Earth targets show partly smooth and partly rough surface with owing the conditions of Equation (1.2) and (1.3). The river and flood regions were recognized as the smooth surface which follows the mirror like reflection (specular direction) of incident electromagnetic wave and signifies the dark colour in the SAR images. Eventually, soil surfaces are related to diffuse scattering element of incident electromagnetic signals of SAR sensor. The backscattering signal direction from soil surface mainly is decided by the dielectric constant and roughness parameters of wet (dielectric constant of approximately 15-30) and dry soil (dielectric constants of approximately 4-6) conditions. As the dielectric constant changes, these changes the strength of backscattering signal which is visualized in the SAR images (Njoku and Kong 1977; Dobson et al. 1985). This is the basic principle of

microwave remote sensing for the analysis of smooth and diffuse region of the Earth's surfaces using various on -board SAR satellite imageries.

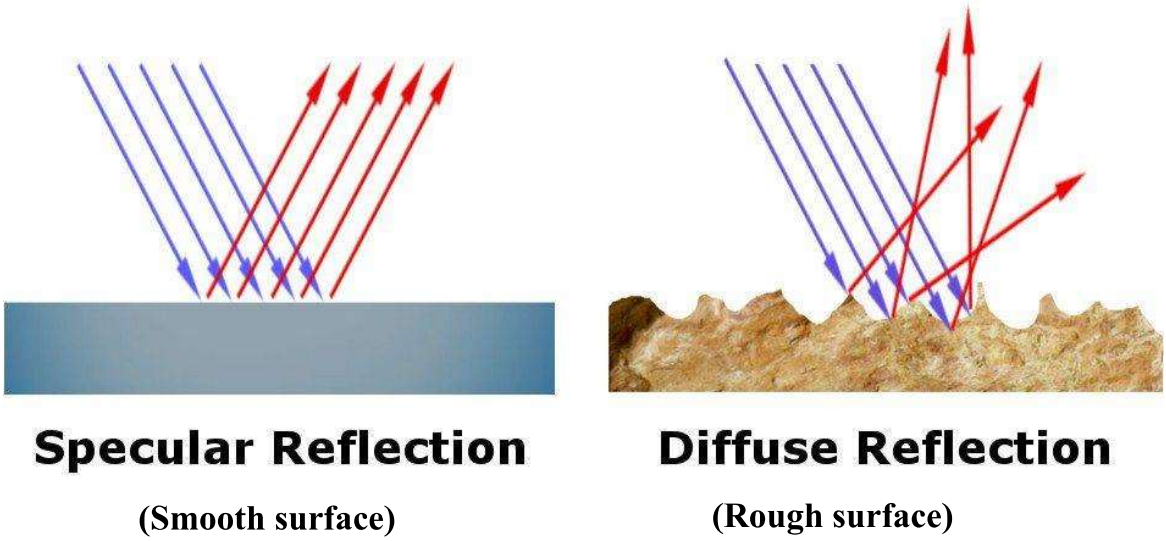


**Figure 1.7 Scattering** mechanism from smooth and rough surfaces

(**Source**: https://i.pinimg.com/originals/7f/14/ba/7f14bab0c6b7b5e0fc9314cb59a350e8.jpg)

**1.7 SYNTHETIC APERTURE RADAR (SAR)**

Synthetic aperture radar (SAR) is a type of active remote sensing techniques for the acquisition of Earth data where a sensor produces its own source of illumination and then records the amount of that energy reflected back toward the SAR sensor after interacting with the Earth features. In the case of SAR, the consecutive time of transmission/reception translates into different positions due to the platform movement. An appropriate coherent combination of the received signals allows the construction of a virtual aperture that is much longer than the physical antenna length. This basic attribute of SAR is the origin of its name "synthetic aperture," giving it the property of being imaging radar. The SAR satellites collect swaths of side-looking signal at a high range resolution and along-track sampling rate to form high resolution imagery. Figure (1.8) shows that the SAR imaging geometry at the Earth surface. The resolution of SAR raw data is defined in two ways:

(I) The **Range resolution ($R_r$)** of the raw radar data is determined by the pulse length (or 1/bandwidth (B)) and the incidence angle. The range resolution is infinite for vertical look angle and improves as look angle is increased. Also note that the range resolution is independent of the height of the spacecraft H. The range resolution can be improved by increasing the bandwidth of the radar. Moreover, the shorter wavelength ($\lambda$) will enable higher bandwidth because the bandwidth is only a small fraction of the carrier frequency.

$$R_r = \frac{c}{2\,B\,sin\theta_a} \tag{1.7}$$

Where c = speed of light, B = band width and $\theta_a$ = look angle

(II) The **Azimuth resolution ($R_a$)** describes the ability of an imaging SAR to separate two closely spaced scatterers in the direction parallel to the motion vector of the sensor. Azimuth resolution is independent of spacecraft height (H) and improves as the antenna length is reduced. Using the synthetic aperture method, the image can be focused on a point reflector on the ground by coherently summing thousands of consecutive echoes thus creating a synthetic aperture perhaps. Proper focus is achieved by summing the complex numbers along a constant range. The focused image contains both amplitude (backscatter) and phase (range) information for each pixel.

However, for real aperture, the azimuth resolution ($d_a$) can be expressed as:

$$d_a = r_0 sin\theta_a = \frac{r_0\lambda}{L} = \frac{\lambda\,H}{L\,cos\theta_a} \tag{1.8}$$

For SAR illumination, the length of aperture is $2d_a$, so the improved azimuth resolution

$$R_a = \frac{r_0\lambda}{2d_a} = \frac{L}{2} \tag{1.9}$$

where $r_0$ slant range, L = aperture length and $\lambda$ = wavelength.

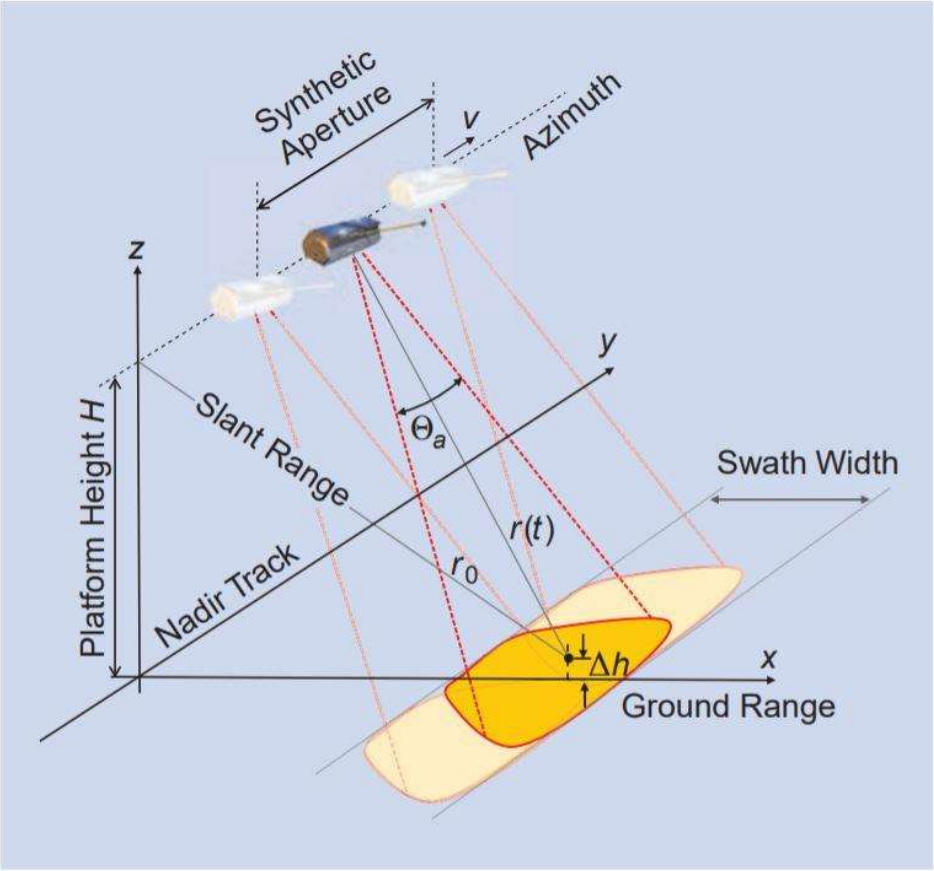


**Figure 1.8** Illustration of synthetic aperture radar (SAR) imaging geometry

The SAR image is most commonly displayed in terms of intensity values such that each image pixel value gives the Fresnel reflectivity of the particular point on the Earth surfaces. The calibration and geo-coding of SAR images has two primary processing steps. The calibration steps ensure that the intensity value actually represents the backscattering signal ($\sigma^0$) value of the reflectivity, i.e., the normalized backscattered intensity within the radar cross section area. The accurate calibration of SAR images is not easy task for considering both sensor calibrations as well as external SAR calibration using Earth targets of known reflected power. The geo-coding refers that the location of any pixel in the SAR image is directly associated to the position on the ground (accurate latitude and longitude value). Typically, the SAR images are geometrically distorted. The reason for this is that the radar only measures the projection of a three-dimensional scene on the radar coordinates,

slant range and azimuth direction. This cause effects such as shadow for areas hidden from the SAR illumination as well as foreshortening and layover manifested by a stretch and compression of sloped terrain.

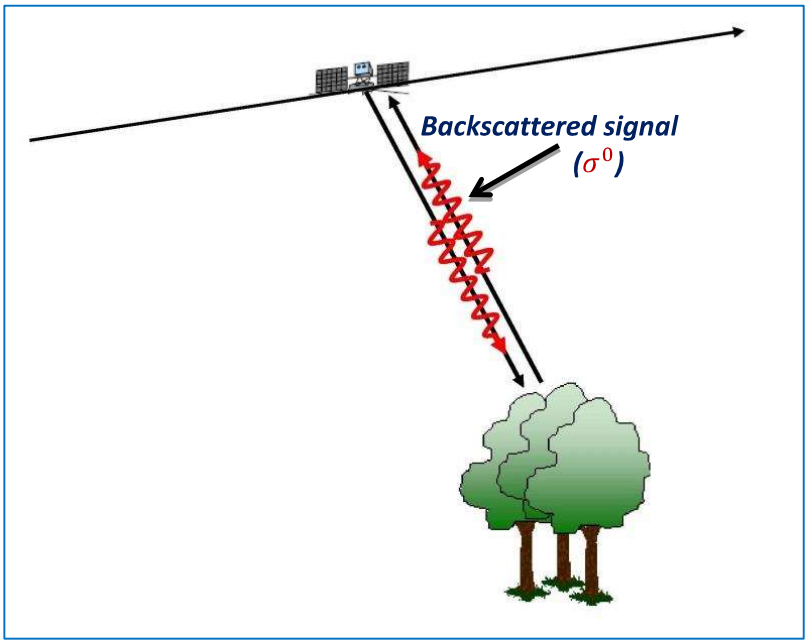


**Figure 1.9** SAR backscattered signal toward the sensor from the vegetation

However, the SAR $\sigma^0$ is defined as the normalised radar return signal recorded from a distributed target and is also called as backscattering coefficient or sigma nought. The Equation (1.10) represents the normalized backscattering coefficient of SAR satellites.

$$\sigma^0 = \frac{4\pi H^2}{\Delta A}\frac{P_s}{P_i} \quad (m^2/m^2) \qquad (1.10)$$

Where ΔA is the area of the illuminated surface over which the phase can be considered constant, H is the SAR-target distance, $P_i$ is the incident power and $P_s$ is the power scattered by the target.

### 1.7.1 Frequency

The potential of SAR signal to penetrate the clouds, precipitation, or land surface cover depends on its frequency. The penetrating power of SAR signal increases with increase of the wavelength (From 1 mm to 1m). If the surface targets size is less than the SAR incident wavelength, then the surface is considered smooth. For example, If the targets fluctuation of the order of 5 cm and ALOS - 2 (L - band) SAR is used, then particular surface or targets appear dark. However, the same surface or targets will appear bright in SAR image at X - band (TerraSAR - X). The L - band has a longer wavelength and having more penetrating power than the C- and X - bands. Due to ability of deeper penetration into the vegetation canopy, the L- band is more useful in forest and vegetation regions. Figure 1.10 shows the microwave frequency regions and classification of frequency used for the various Earth surface features (vegetation, soil, snow and ocean). For vegetation and soil monitoring, the commonly used frequencies are L-, C- and X- bands. The ample research has been carried out for more accurate monitoring and retrieval of parameters using on-board multi-orbiting SAR satellites (RADRASAT - 2, Sentinel - 1A, ALOS - 2 and TerraSAR - X). These bands have been successfully monitoring the crop growth and soil surface parameters estimation.

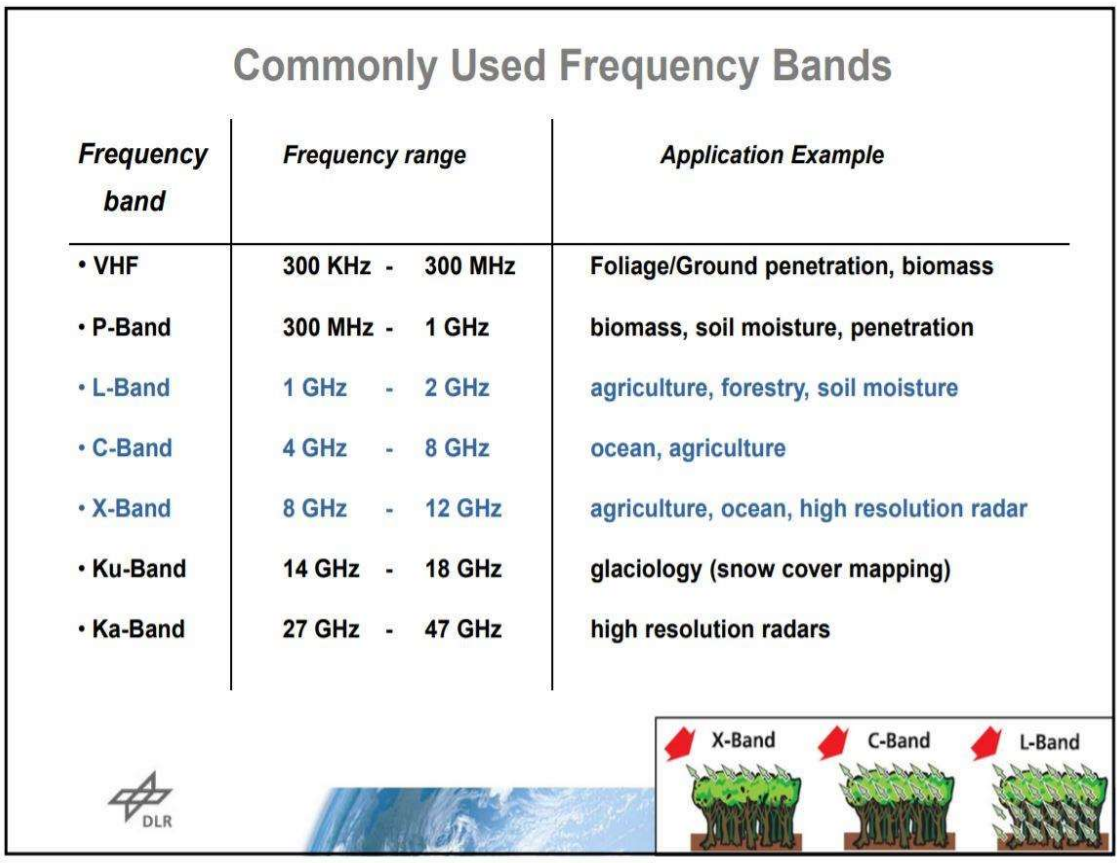


**Figure 1.10** Microwave frequency bands and their application

### 1.7.2 Polarization

The SAR signal is polarized wave. The polarisation of SAR signal is decided by the orientation of the electric field vector of the transmitted signal with respect to the Earth surface. If the electric field vector direction is parallel to the Earth surface, the signal is referred to be "**H**" polarised. Whereas, the "**V**" polarisation occurs if the electric field vector direction is perpendicular to the Earth surface. Figure 1.11 shows the SAR electric wave vector illuminating energy on the Earth features. When the incident electric wave vector interacts with the Earth targets, the polarisation state may be altered (depolarization of wave vector). Therefore, the SAR backscattered echoes usually have a combination of the two polarisation states. The SAR sensors are designed to detect the **H** or the **V** component of the backscattered signal from the Earth targets. Hence, the four possible polarisation

combinations are possible of SAR system: (I) **HH**: Horizontal transmit, Horizontal receive (II) **HV**: Horizontal transmit, Vertical receive (III **VH**: Vertical transmit, Horizontal receive and (IV) **VV**: Vertical transmit, Vertical receive). Since, on the basis of polarization, SAR satellites are categorized into two ways: (I) Dual polarization (VV +VH or HH + HV) (II) Quad- polarization (HH + VV + HV + VH). The study of all the SAR polarization state is equally important for physical characterisation of the Earth targets. Till now, the various on-board SAR satellites are orbiting in space platform under the various Earth observation missions. For example, TerraSAR - X/TanDEM - X (dual and quad polarizations), RADARSAT-2 (HH + VV + HV + VH), ALOS -2 (HH + HV or quad polarization) and Sentinel - 1A (VV + VH) SAR are orbiting in different polarization beam mode.

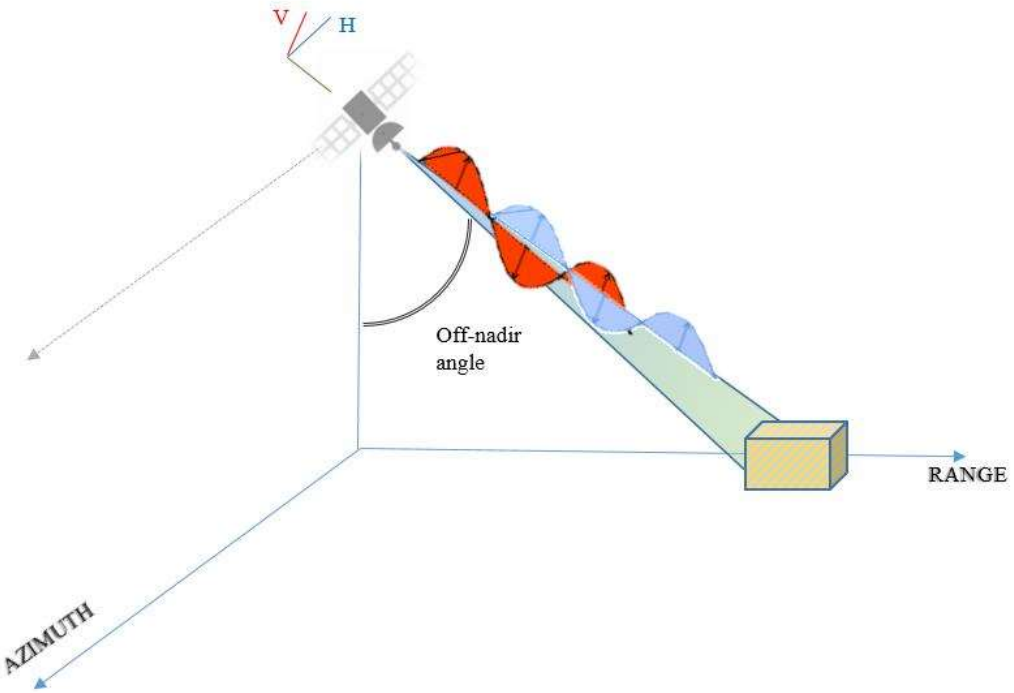


**Figure 1.11** Electric wave signal interaction at the Earth target with horizontal (H) and vertical (V) polarization of EM wave

### 1.7.3 Incidence angle

The SAR looking incidence angle (θ) is defined as the direction of illumination of the SAR signal and the Earth surface plan (Figure 1.12). The interaction between SAR incident signal and the surface depends on the θ of the SAR pulse on the surface. The θ depending on the height of the sensor. Therefore, the local inclination of the surface influences the SAR image brightness. However, the RADARSAT - 2 (C - band) is the first space-borne SAR which senses the Earth surface at different incident angles and resolutions. The Sentinel-1A (C - band) and ALOS - 2 (L - band) have incidence angle range $25^0$ - $43^0$ and $8^0$ - $70^0$, respectively. The larger incident angle may be more suitable for other applications. For example, a large incident angle will increase the contrast between the forested and open areas (non-forest).

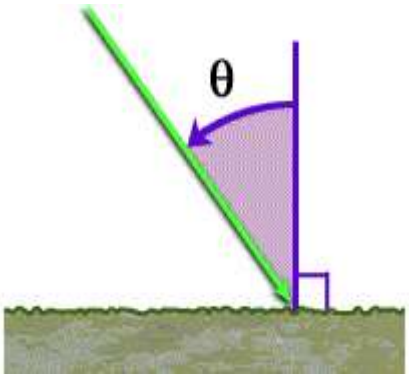


**Figure 1.12** SAR looking incidence angle

However, the Figure (1.13) shows the backscattering values ranging from lower to higher values under the different typical Earth features. The SAR system (frequency, polarization, incidence angle) and surface parameters (dielectric constant, roughness) are responsible for the variation of $\sigma^0$ (dB). Generally, the -10 dB to -20 dB values are associated for crops (moderate crop) and -10 dB to -5 dB values correspond to very rough surface or dense vegetation (forest canopy). However, urban areas and extreme rough surface showed the double bounce effects which causes the higher backscattering values (above -5 dB).

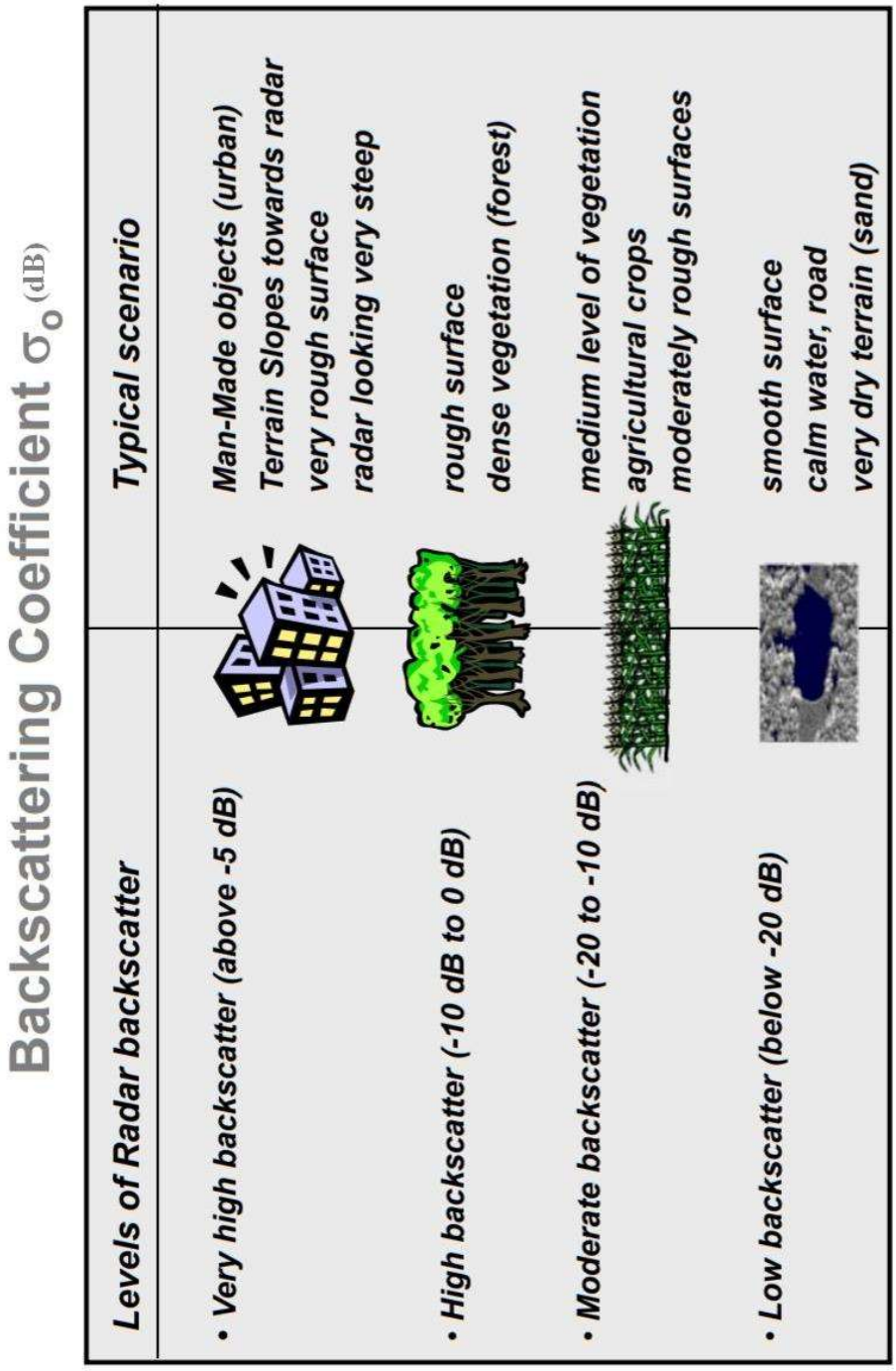


**Figure 1.13** Classification of backscattering coefficient ($\sigma^0$) for various features at the Earth surface

(**Source:** Jet propulsion laboratory (NASA))

## 1.8 APPLICATIONS OF OPTICAL AND MICROWAVE REMOTE SENSING

The optical and microwave remote sensing are complementary for precise monitoring of the natural and man-made activities at the Earth surfaces. The optical remote sensing satellite data has ability to greatly discriminate the crops, forestry and urban regions in the imagery. The vegetation at the Earth surface is very sensitive in the EMR from RED to NIR region. The optical images are being contaminated or not more useful for Earth observations during the rainy season, haze and cloudy conditions in the atmosphere. The strength of microwave signal (longer wavelength) are: (i) it can easily penetrate the atmospheric haze, (ii) gets least influenced (almost negligible) in the cloudy and raining seasons and (iii) has day-night imaging capability. Moreover, the microwave remote sensing is useful for the monitoring of snow and ice needed for meteorological and climate research, hydrological purposes (soil moisture) and navigation and offshore activity in polar regions. The study on inter planetary surfaces is one of the great achievements which helps in identification of surface materials, rock types, water etc. using satellite images. Figure 1.14 shows the other major areas of Earth features where both optical and microwave remotely sense imagery and technology play important role for forecasting the disaster risk and monitoring the natural activities. Thus, the remote sensing has great potential for various applications and the following list provides example of some areas where it is used prominently.

- Agriculture practices and management
- Forestry
- Geosciences
- Vegetation monitoring
- Soil moisture estimation
- Drought monitoring

- Land use/land cover
- Volcanic activity monitoring
- Environmental modelling
- Seismology
- Oceanology
- Glaciology
- Monitoring of atmospheric constituents
- Biodiversity conservation

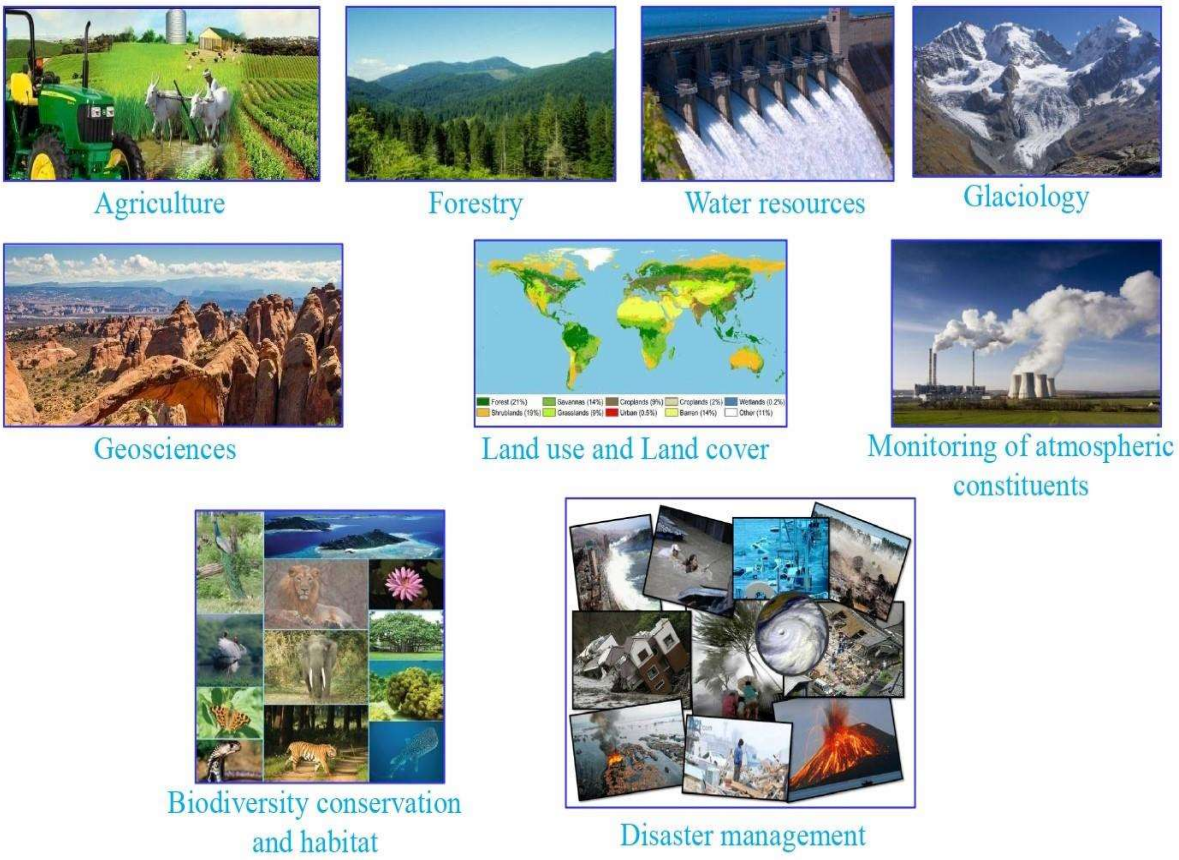


**Figure 1.14** Illustration of optical and microwave remote sensing applications

(**Source:** Jet propulsion laboratory (NASA))

## 1.9 REVIEW OF LITERATURE

Biophysical parameters retrieval of crop using microwave and optical remote sensing data would be essential considering their correlations with system parameters (wavelength, polarization and vegetation indices) and change in phenological variation (Borchani et al. 2015). Among the optical and SAR Earth observation sensors, the SAR data showed great potential for vegetation monitoring due to its unique characteristics (polarizations, frequencies and incidence angle) and sensitivity to geometric and dielectric properties of the Earth targets (Ulaby 1975; Steele-Dunne et al. 2017). SAR backscattering intensity from the vegetation canopies is often dependent on the radiative transfer models of direct and indirect measurable crop biophysical parameters (Ulaby et al. 1990; Karam et al. 1995; De Roo et al. 2001; Graham and Harris 2003). Till now, the ample studies have been carried out to retrieve crop biophysical parameters from SAR data at different polarizations and frequencies (X-, C- and L- bands). Attema and Ulaby (1978) developed the semi-empirical water cloud model (WCM) for retrieval of the vegetation parameters using electromagnetic wave theory. Thus, the WCM is expected to be well adapted for the operational monitoring and retrieval of biophysical parameters. A large number of research articles have been (Inoue et al. 2014; Chakraborty et al. 2005; Dabrowska-Zielinska et al. 2007; Bériaux et al. 2015; Hosseini et al. 2015; Hosseini and Heather 2017) reported for the robustness of WCM for biophysical parameter estimation for several crop types at different SAR system parameters. These results suggest the further modification of the WCM needed for acceptable accuracies and its scalability to retrieve the crop biophysical parameters.

Xie et al. 2019 studied the winter wheat crop biophysical parameters retrieval from Sentinel -2 imagery using various Red -Edge indices based models and radiative transfer model (RTM). The main focus of this research to retrieve the leaf area index (LAI), leaf chlorophyll content (LCC) and canopy chlorophyll content (CCC). The ANN and LUT based

combined physical inversion approach was adopted in the developed semi-empirical indices model for the retrieval of winter crop growth parameters. They found that the hybrid inversion modelling was more robust than iterative optimization (IO) or traditional optimization algorithms. Also, this study investigated that the Red-edge indices are more sensitive for various crop growth stages than the other visible range indices (like NDVI and MSR).

Meanwhile, some limited studied have been performed for the monitoring the crop biophysical and soil parameters using synergetic use of optical and SAR satellite data. Since, the optical and SAR are complementary to each other for more precise monitoring of Earth observations from the space platform. The Indian agriculture and around the world, the monsoon crops (mainly Rabi and Kharif seasons) play vital role in economy growth and food security. Therefore, the recent advances of orbiting satellite (viz. Sentinel -1A and Sentinel -2) at fine spatio-temporal resolutions have proven great ability for identification of crops growth, soil moisture and drought condition more accurately. The synergy of both SAR (Sentinel - 1A) and optical (Sentinel - 2) satellite data potentially monitor the vegetative/non - vegetative cropland and also enrich the development of direct/ indirect algorithms (Van Tricht et al. 2018; Qadir and Mondal 2020). Zhao et al. (2020) demonstrated the synergetic use of both Sentinel -1A and Sentinel -2 for accurate monitoring the cropland at various stages of its phenology. Optical satellite images often get contaminated by the cloud cover or haze in the atmosphere which may restrict the time-series study of crops and their growth parameters monitoring. Thus, they developed the Multi - CNN-Sequence to Sequence (MCNN - Seq) model and formulate the correlation between the optic and SAR time series sequence algorithms to lift overcome this problem. Gao et al. 2017 studied the synergetic use of Sentinel-1 and Sentinel-2 satellite data for soil moisture retrieval and mapping at 100 m

resolution. They developed the two methodologies (NDVI triangle methods) for the mapping of soil moisture at fine scale.

Soil physical or empirical/semi-empirical models are generally developed on the basis of wave theory of EMR, and the validity of these models is limited to different wavelength regions and surface roughness conditions (Fung et al. 1992). Moreover, the developed physical models include the two type of approximation model (1) Small perturbation model (SPM) valid for lower frequency regions (2) the Kirchhoff models (KM) valid for higher frequency regions. Further, based on surface soil geometry, the KM is divided into two parts called the Physical optics model (POM) and the Geometrical optics model (GOM), which are applicable to high frequency regions (Ulaby et al. 1982). Fung et al. (1992) developed the Integral Equation Model (IEM) that combined Kirchhoff and Small perturbation models and hence are valid for wider frequencies range and surface roughness parameters. Chen et al. (1995) simplified the IEM by including the minimum system and surface parameters at different polarizations (HH and VV) and various soil moisture conditions (dielectric constant). This approach helped to reduce the complexity of inversion of developed IEM. Bindlish and Barros (2000) retrieved the soil moisture by the IEM model using the inversion algorithm (LUT) at multi-frequency and multi-polarization data of space-borne SAR. Oh (2004) demonstrated the semi-empirical polarimetric soil backscattering model for the estimation of soil moisture and surface roughness parameters from multi-polarized radar data. The co polarization ($P = \frac{\sigma^0_{HH}}{\sigma^0_{VV}}$) and cross polarization ($q = \frac{\sigma^0_{VH}}{\sigma^0_{VV}}$ ) ratio values were jointly used for more accurate inversion of the developed model for robustness of soil moisture accuracy. Also, he analysed that the main source of error of electromagnetic signal of radar arises due to the surface roughness parameters, which hampered the correlation between the soil moisture and the radar backscattering coefficient.

Generally, the physical and empirical models of soil can infer the behaviour of the backscattering coefficient with the changes in surface roughness and soil moisture (Dubois and van Zyl 1994). However, their applicability is limited due to the complex and restrictive requirement for the parameterization of the vegetation and soil surface layer. This causes hindrance in soil moisture estimation (Ulaby et al. 1986). Now, the various inversion or hybrid inversion algorithms were developed to solve this ill-posed problem. Zhu et al. (2019) evaluated the multi-frequency framework for soil moisture retrieval from time-series radar data. In this study, the L - band airborne data, C-band RADARSAT-2 data and X-band COSMO-SkyMed data were used for configuration of numerical inversion techniques (NMM3D). The NMM3d approach builds the non-parametric (machine-learning) and LUT algorithms. Hence, they reported that this hybrid inversion method (NMM3D) inverts the soil scattering algorithm more accurately and offers the high correlation and low RMSE with in-situ soil moisture.

In the new era of microwave remote sensing, the polarimetric SAR (PolSAR) and polarimetric interferometric SAR (PolInSAR) have emerging techniques to study the land cover classification analysis. Moreover, the PolInSAR is complementary to PolSAR information and that both are essential for producing accurate land cover classification and retrieval of its parameters. PolSAR techniques are greatly involved to the generalization of electromagnetic wave theory and improved the science of microwave remote sensing for the Earth observations (Erten et al. 2019; Uppala et al. 2019; Mandal et al. 2019; Mandal et al. 2020). The vegetation and soil remote sensing applications greatly covered by PolSAR data due to diversity of scattering physics. PolSAR methods totally depend on coherent scattering vectors echoes from the vegetation or soil surfaces (Shimoni et al. 2009; Tao et al. 2017). These two methods (PolInSAR and PolSAR) required the dual polarimetric (HH +HV or VV + VH) or quad-polarimetric (HH + VV + HV + VH) SAR data.

Mandal et al. (2020) studied the polarimetric radar vegetation index over the various crops (Soyabean, Canola and wheat) using the Sentinel - 1A SLC (central frequency 5.405 GHz) data. They utilized the 2 × 2 covariance scattering matrix for computation of radar vegetation descriptors. The polarimetric decomposition algorithm (Unitary transformation) was adopted to compute the eigen-values of covariance matrix, which mainly describes the dominancy of scattering mechanism. Also, they used the degree of polarization (developed by Barakat, 1977) for modification of radar vegetation index. However, the dual polarimetric radar vegetation index (DpRVI), polarimetric radar index (PRVI) and radar vegetation index (RVI) were utilized for the potential of radar index to the estimation of crop biophysical parameters. The plant area index (PAI), vegetation water content (VWC) and dry biomass (DB) crop growth parameters were retrieved by inversion of methodology at dual channel (VV + VH) of polarimetric SLC data. The statistical performance indices showed that the DpRVI having better correlation with reported crops and their biophysical parameters than PRVI and RVI. Notably, the proposed study has investigated the potential of radar vegetation indices and it is motivated to researcher/scientist for further development of radar indices using higher wavelength (L- and P- bands) at HH + HV polarization. Also, encourage to develop the radar vegetation index at higher order covariance matrices (3 × 3 and 4 × 4) and coherency matrices ($T_3$ and $T_4$).

However, the developed models and the experimental researches on vegetations and soil have been completely focused on the either optical or SAR system. The synergetic configurations of the SAR, optical system and polarimetric SAR (PolSAR) indices for Earth surface observations have recently become a subject of interest. The limited studies were performed in the coupled form of vegetation and soil microwave scattering algorithms using SAR and optical satellite data. Due to availability of recently launched spatio-temporal on-board SAR satellite at various frequency ranges and multi polarizations (dual- and quad-

polarizations), the PolSAR techniques are greatly employed in the study of crop and soil parameters monitoring. In the case of the Pol-SAR, the SLC data are required to study the vegetation dynamic using n × n covariance scattering matrix (Barakat, 1977). The advantages and disadvantages of the SAR over the optical system are given below:

1. SAR backscattering coefficients are more sensitive to the vegetation and soil parameters than that of the optical indices (Zhang et al. 2016; Qadir et al .2020).

2. SAR backscattering coefficients do not show extreme saturation effect with the increasing the crop growth stages and have better sensitivity than optical satellite data (Zhang et al. 2016; Kumar et al. 2018; Qadir et al .2020).

3. The SAR signals are more sensitive for soil moisture retrieval than optical data. But the synergy of both systems may increase the accuracy of microwave algorithms (Ceraldi et al. 2005; Baghdadi et al. 2009).

4. Radar vegetation indices have more potential to get multi-dimensional information about the vegetation and soil surface due to the diversity of SAR sensor configuration (Mandal et al 2020).

5. The Pol-SAR study mainly occurs in the microwave region which enhances the understanding of physical scattering of Earth features (vegetation, soil, urban and water) than SAR backscattering and optical responses.

The main drawback of the optical satellite data is its operational difficulty in rainy and cloudy season for acquisition on the Earth target of interest which create the data gap (due to contaminated pixels). Therefore, the synergetic use of optical and microwave satellite data are required to bridge the gap for acquiring complementary information for vegetation and soil monitoring more accurately from the space platform. The PolSAR techniques for crop growth study are more complicated than the SAR and optical system, which requires more understanding about the scattering mechanism for the vegetation and soil layers.

## 1.10 MOTIVATION OF STUDY

A considerable quantity of theoretical and experimental research for Earth surface observations (viz. vegetation and soil surfaces) have been carried out by using the airborne and space-borne platform sensors. Various research have been carried for improving the monitoring algorithms for crops and soils using optical and microwave satellite data for different crops and soil conditions. But complexity of backscattering physics over vegetation and soil layers are still challenging task for the development of operational algorithm that reduces the reasonable errors in satellite data products. Therefore, the finer spatio-temporal mapping of crop growth stages and soil moisture has become a major priority for researcher around the world using multi-sensor satellite data. However, the following research problems motivated to this study which primarily aim to enrich the scientific knowledge and diversity of backscattering physics.

Remote sensing satellite images provide information about the crop growth parameters at different phenological stages for assessing the crop health and stress conditions as and when needed. Although, some disadvantages of optical satellite data during cloud cover and rainy season, the SAR satellite images have been proven remarkable tool for precise study of crop growth and soil conditions. Since, the SAR backscattering coefficients of the various targets under study involve large number of system and target parameters, which complicates the inversion of the developed model for the retrieval of biophysical parameters (Picard et al. 2003; Ferrazzoli et al. 2000; Picard et al. 2003). Cookmartin et al. (2000) developed a multilayer second order radiative transfer model (RTM) and consider the attenuation factor of every layer for the inversion formulation, which resulted in complex expressions for retrieving the vegetation parameters. Multiple coherent scattering models were developed for understanding the SAR backscattering over crop canopy at different polarization and frequency (X-, C-, and L- band).

The study of multiple scattering interactions complicates the microwave scattering algorithms and hence, it hampered the accuracy of the inversion of the biophysical parameters. Therefore, it is required to develop robust algorithm which requires least system and target parameters and may easily be inverted for the retrieval of biophysical parameters and soil moisture. These problems of inversion may be overcome by using hybrid algorithm (machine learning and parametric optimization techniques).

In the recent era of remote sensing technology, the polarimetric SAR (PolSAR) study plays vital role to understand the scattering mechanism (first order, second order and higher order) from vegetation and soil surfaces. The coherency ($T_3$ and $T_4$) and covariance ($C_2$ and $C_4$) scattering matrix depend on the dual and quad -polarization beam mode. The limited studied have been performed on PolSAR using electromagnetic wave theory (degree of polarization and state vector). The availability of RADARSAT - 2 (HH + VV + HV + VH), Sentinel - 1A (VV + VH) and ALOS - 2 (HH + HV or HH + VV + HV + VH) operational SAR data have motivated the researchers to explore the novel vegetation and soil scattering algorithm and radar index to enrich the backscattering physics from vegetation and soil layers.

Remote sensing data acquired by Landsat - 8 (OLI), Sentinel - 2, Sentinel – 1A, ALOS - 2, MODIS and PROBA - V satellites have been used in this research work. The potential of all the above satellite data have not been explored much for monitoring and retrieval of biophysical parameters and soil moisture in the high order backscattering modelling for complex vegetation and soil interfaces. The synergetic use of Sentinel - 1 A (C - band) and ALOS - 2 (L - band) have not been investigated much for biophysical and soil parameters retrieval over the Indian agroclimatic zones.

The outcomes are of substantial scientific and practical values to the broader remote sensing community and research studies for biophysical parameter and soil moisture retrieval.

The modelling approach suggested in this study is expected to provide more accurate and rapid monitoring of agricultural crops and soil moisture conditions. This research work may also be useful for agro-meteorological and crop monitoring managements at different observational scales using optical and SAR time-series remote sensing images.

## 1.11 RESEARCH QUESTIONS

The present research work being performed for modelling and monitoring of SAR backscattering signal from the vegetation and soil surfaces and retrieval of their parameters (biophysical and soil moisture). Furthermore, some research questions have to be answered as shown below:

1. How can the developed Red-edge vegetation descriptors computed from Sentinel-2 satellite at finer spatial resolution be more accurate simulation of backscattering coefficient ($\sigma^0$) for forward modelling vegetative covered areas?
2. How to $f_{veg}$ in the modified water cloud model (MWCM) weighted the vegetation and soil fraction within a pixel and reduce the complexity for retrieval LAI of wheat crop using time-series Sentinel -1A SAR satellite data?
3. How can the synergy of vegetation and soil microwave scattering algorithm be more robust for accurate retrieval of LAI?
4. How to improve the coupling of an improved inversion algorithm and soil scattering modelling for spatio-temporal mapping and retrieval of soil moisture?
5. How can polarimetric radar vegetation index (2 × 2 covariance scattering matrix) be more sensitive in the microwave scattering algorithm as vegetation descriptor for simulation of backscattering responses from the vegetation canopies using Sentinel - 1A (VV + VH) and ALOS - 2 (HH + HV) SAR data at different frequency (C and L - band).

## 1.12 RESEARCH OBJECTIVES

The research work performed and presented in this thesis focuses on modelling of the backscattered signal from vegetation and soil surfaces using synergetic use of optical and SAR satellite data. The modified or developed microwave scattering algorithm improves the monitoring and retrieval of their parameters (biophysical and soil parameters). Moreover, the potential of the dual polarimetric radar vegetation index at HH + HV and VV + VH polarizations was evaluated in the higher order microwave vegetation scattering model. The specific research objectives of this thesis are as below:

1. Assessment of Red - Edge derived vegetation descriptors (red edge wavelength regions) in modified water cloud model (MWCM) using Sentinel - 1A and Sentinel - 2 satellite data.
2. The time – series study of LAI for wheat crop were quantified using the modified microwave scattering algorithm and scale invariant vegetation fraction ($f_{veg}$).
3. The synergetic vegetation and soil microwave scattering algorithm were developed for fine spatio – temporal mapping and retrieval of biophysical parameter using Sentinel - 1A SAR satellite data.
4. An improved inversion algorithm was devolved for retrieval of more accurate soil moisture by coupling of machine learning techniques and modified soil scattering algorithm.
5. Dual polarimetric radar vegetation indices were assessed in high order scattering algorithm which computed from 2 × 2 covariance scattering matrix using Sentinel - 1A (VV + VH) and ALOS - 2 (HH + HV) SAR satellite data.

The performance of microwave scattering algorithm is based on the physical scattering of vegetation and soil surface, vegetation descriptors, optimization algorithm and inversion

algorithm. Therefore, the different optical and SAR vegetation descriptors were used in the modified microwave scattering algorithm for the retrieval of biophysical and soil moisture.

## 1.13 ORGANISATION OF THESIS

In the present thesis, the modelling and monitoring of SAR backscattering responses ($\sigma^0$ (dB)) were carried out for the retrieval of biophysical parameter and soil moisture in the vegetative and non-vegetative cover fields. The co- polarization (VV) and cross polarization (VH) Sentinel - 1A SAR (C - band) and optical (Landsat - 8, Sentinel - 2, PROBA - V and MODIS) satellite images were used in this research work. The vegetation and soil microwave scattering algorithms or some modified models were developed for accurate mapping and retrieval of crop growth parameter (LAI) and soil parameter at fine spatio-temporal using complementary information computed from optical satellite data (i.e., $f_{veg}$).

**Chapter 1** pertains to describe the introductory background of remote sensing techniques and brief review of some research work carried out for modelling and monitoring the crops/vegetations and soil surfaces by retrieval of biophysical parameters, soil moisture using physical, empirical and semi-empirical algorithms and different computational techniques.

**Chapter 2** pertains to describe an experimental procedure for the computation of LAI and soil moisture, root mean square height (s) and correlation length (l) during in-situ measurements. It was also discussed about the details computation of $\sigma^0$ (dB) from SAR and different spectral indices (NDVI and Red - Edge Indices) form optical satellite data. Furthermore, the backscattering mechanism from vegetation canopy, soil surfaces and intermediate effect (multiple scattering from vegetation and soil layers) was described.

**Chapter 3** In this chapter, the Red-Edge vegetation descriptors computed from Sentinel - 2 was assessed in a modified water cloud model (MWCM) for forward modelling using Sentinel - 1A SAR satellite data. The soil geometrical model was incorporated for

computation of soil backscattering according to soil roughness and moisture condition. The modified Beer's law was selected for the development of vegetation descriptors using various optical indices. The Red - Edge normalized difference vegetation index ($NDVI_{RE}$) performed robust optical index in Red - Edge spectral interval to simulate the higher accuracy in forward direction. The lower value of computed root mean square error (RMSE), higher correlation ($R^2$) and better NSE between the SAR derived and simulated $\sigma^0$ (dB) values showed high potential of developed index for the forward simulation modelling from the vegetation and soil layers.

**Chapter 4** pertains to describe the retrieval of LAI of wheat crop using time-series Sentinel -1A and Sentinel - 2 satellite data at co-polarization (VV) and cross polarization (VH) channels of EMR signal. The MWCM and WCM semi-empirical models were evaluated for the robustness of modified vegetation model. The optimized unknown model parameters were computed using hybrid non- linear least square optimization algorithm at 95 % confidence level using training data sets. After the calibration of the MWCM, the modelled $\sigma^0$ (dB) values were simulated at VV and VH channels. The results indicated high potential of the developed MWCM to provide the improvements in simulated $\sigma^0$ (dB) than that of old WCM at both polarizations. However, the LUT based inversion algorithm was applied for the retrieval of LAI for wheat crop at VV and VH polarizations. Therefore, performance indices ($R^2$, RMSE and bias) authenticated the MWCM can be applied successfully to retrieve the LAI of wheat crop. The estimated values of LAI by MWCM were found to show better correlation than those values of LAI obtained by WCM at VV and VH polarizations. The MWCM provides a substantial tool for the retrieval of biophysical parameters for wheat and barley crops by combining the potential of SAR and optical data. However, due to all weather acquisition capability, better temporal resolution of SAR satellite data, the potential of the

MWCM needs to be further verified at different polarizations (HH and HV) and frequencies (L -, X -, S - bands in the microwave regions).

**Chapter 5** In this chapter, the modified synergetic backscattering model of vegetation (i.e. MWCM) and direct scattering model of soil (i.e. MSSM) were developed for the retrieval of LAI over wheat and barley crops using C- band (5.405 GHz) Sentinel -1A images and scale invariant $f_{veg}$ parameter computed from Landsat-8 data. The non-linear least square optimization (constrained with derivative Jacobian matrix) technique was established for calibration of proposed methodology. The inverse modeling results indicated a high potential of the proposed modified synergetic algorithms to retrieve LAI more accurately at finer spatio-temporal resolutions than the older developed semi-empirical and empirical approaches. In the forward modeling, the simulated $\sigma^0(dB)$ at VV polarization of the synergetic algorithm was found better than that of VH polarization. However, the retrieval performance of LAI values for inverse modeling scheme indicated higher $R^2$ and lower RMSE relationship with in-situ measurements at VV channel than that of well-established on-board PROBA - V and MODIS LAI satellite products. Therefore, this synergetic form of MWCM and MSSM model may provide a new tool for the more accurate mapping of biophysical parameters by coupling the recent advances of SAR and optical satellite data from space platform. Moreover, due to the limitation and unavailability of fine spatial and temporal resolution LAI satellite data product, this modified developed algorithm could be used as an alternative approach to estimate the LAI over agricultural fields for ongoing and future SAR satellites missions.

**Chapter 6** pertains to evaluate the potential of C - band SAR and developed improved inversion algorithms for the accurate mapping and estimation of soil moisture ($M_v$) in two type of regions (vegetative and sparse-vegetative covered field). The semi-empirical MWCM backscattering model was developed by incorporating $f_{veg}$ and LAI as vegetation parameters

for the retrieval and mapping of $M_v$. The $f_{veg}$ were computed using Landsat-8 satellite data in the vegetated and sparse vegetated soil sample fields. After the calibration of the MWCM, the MTRFR inversion algorithm was used for the retrieval of $M_v$ in the study regions - 1 and - 2 during all the temporal changes followed by LUT techniques. The MTRFR algorithm has more capability to reduce the outlier noise and required minimum hyper-parameters as compared to others inversion algorithms like iterative optimization (IO), ANN and SVM. Therefore, the MTRFR based inversion algorithm developed in the present thesis provided the better inversion tool as compared to inversion techniques applied in recent past to MWCM for the estimation of $M_v$. The results and statistical evidence have proven high potential of the developed semi-empirical MWCM and improved inversion process to retrieve and map the spatio-temporal patterns of $M_v$ more accurately using time-series Sentinel - 1A SAR data, which may become more time continuous with the constellation of Sentinel - 1A and Sentinel - 1B satellites in the near future.

**Chapter 7** In this chapter, the new and more emerging techniques were incorporated in the high order microwave backscattering algorithm for the mapping and simulation of forward backscattered using dual polarimetric radar vegetation (DpRVI) and radar vegetation index (RVI). The 2 × 2 covariance matrix ($C_2$) was generated from the dual polarimetric Sentinel - 1A SAR satellite data. The eigen-decomposition method was adopted for computing the non- negative eigen values ($\lambda_1$ and $\lambda_2$) of $C_2$ matrix. The eigen values quantify the dominancy of scattering mechanism from first order (VV polarization of direct scattering with no multiple scattering) and second and higher-order scattering (VH polarization with two or more reflections). The developed algorithm was parameterized using high and more robust Genetic optimization algorithm technique (GOAT). The retrieval results of simulated biophysical variable from the developed high order backscattering algorithm demonstrated

better performance of DpRVI than RVI as vegetation descriptor in microwave scattering algorithm.

**Chapter 8** pertains to describe the conclusions and future prospective of the research work of the present thesis. We envisage that this research would be able to develop more robust operational algorithms to retrieve the crop and soil parameters form the space-borne and air-borne sensors more authentically than ever before. The developed synergetic algorithm with coupled C - band SAR and hybrid computational methods have added a new dimension to enhance the inversion accuracy and biophysical parameter retrieval accuracy which led to clear understanding of remote sensing application over crop land using upcoming sensors from space platform in near future. Conclusions drawn through this research work will find tremendous application in agriculture monitoring, agro-meteorology and various agricultural missions (especially in our Indian perspective). Also, the further research work will be continuing to other dual polarimetric (HH and HV) ALOS - 2 satellite data and quad-polarimetric (HH, VV, HV and VH) RADARSAT - 2 satellite data. The high order covariance matrix ($C_2$ and $C_4$) would be generated for more accurate study of complex scattering from Earth targets (i.e. vegetation and soil surfaces) and develop the novel radar vegetation index (NRVI) as a robust vegetation descriptor in microwave scattering algorithm using on-board L -, C - and X - band SAR satellite data.